

A Catalogue of Morphologically Classified Galaxies from the Sloan Digital Sky Survey: North Equatorial Region

Masataka Fukugita^(a,b), Osamu Nakamura^(c), Sadanori Okamura^(d), Naoki Yasuda^(a),
John C. Barentine^(e), Jon Brinkmann^(e), James E. Gunn^(f), Mike Harvanek^(e),
Takashi Ichikawa^(g), Robert H. Lupton^(f), Donald P. Schneider^(h), Michael A. Strauss^(e),
Donald G. York⁽ⁱ⁾

^(a)*Institute for Cosmic Ray Research, University of Tokyo,
Kashiwa 277 8582, Japan*

^(b)*Institute for Advanced Study, Princeton, NJ 08540, USA*

^(c)*Graduate School of Political Science, Waseda University, Shinjuku, Tokyo 169 8050,
Japan*

^(d)*Department of Astronomy, University of Tokyo, Hongo, Tokyo 113, Japan*

^(e)*Apache Point Observatory, Sunspot, NM 88349, USA*

^(f)*Princeton University Observatory, Princeton University, Princeton, NJ 08544, U. S. A.*

^(g)*Astronomical Institute, Tohoku University, Sendai 980 8578, Japan*

^(h)*Department of Astronomy and Astrophysics, Pennsylvania State University. University
Park, PA 6802, USA*

⁽ⁱ⁾*Department of Astronomy and Astrophysics, University of Chicago, Chicago, IL 60637,
USA*

ABSTRACT

We present a catalogue of morphologically classified bright galaxies in the north equatorial stripe (230 deg²) derived from the Third Data Release of the Sloan Digital Sky Survey (SDSS). Morphological classification is performed by visual inspection of images in the g band. The catalogue contains 2253 galaxies complete to a magnitude limit of $r = 16$ after Galactic extinction correction, selected from 2658 objects that are judged as extended in the photometric catalogue in the same magnitude limit. 1866 galaxies in our catalogue have spectroscopic information. A brief statistical analysis is presented for the frequency of morphological types and mean colours in the catalogue. A visual inspection of the images reveals that the rate of interacting galaxies in the local Universe is approximately 1.5% in the $r \leq 16$ sample. A verification is made for the photometric catalogue generated by the SDSS, especially as to its bright end completeness.

Subject headings: galaxies: fundamental parameters (classification) – catalogs

1. Introduction

This paper presents a catalogue of morphologically classified galaxies from the Sloan Digital Sky Survey (SDSS: York et al. 2000), Data Release Three (DR3; Abazajian et al. 2005). We limit our sample to a rectangular region of the equatorial area in the Northern sky (R.A. $\approx 9^h.7 - 15^h.7$) of 230 square degrees that comprises 2658 objects brighter than the r band Petrosian magnitude $r_P \leq 16$ that are listed as extended in the DR3 photometric catalogue. The classification is performed by visual inspection by three people independently, and the final classification is obtained from the mean. We obtain a sample of 2253 galaxies, of which 1866 have spectroscopic information in the SDSS.

Visual classification is a labourious and somewhat subjective procedure. Nevertheless, this remains the best approach to classify each galaxy into a Hubble type with high confidence, at least for bright galaxies. There are a number of methods that use photometric and/or spectroscopic parameters developed for large scale samples to classify galaxies. Those classifications are correlated reasonably well with visual Hubble types, but are substantially contaminated by galaxies that belong to obviously wrong classes if visual inspection is made. The identification of Sa galaxies is particularly subtle. The classification of Sa galaxies often scatters across elliptical to late spiral galaxies, if one uses photometric and/or spectroscopic parameters as indicators. On the other hand, it is not difficult to identify disks of Sa galaxies with visual inspection. Colour or spectroscopic parameters are sensitive to the star formation activity, so galaxies that show such activities are typically classified as a late type if those parameters would be used. For the moment it is difficult to replace the classification with a quantitative measure.

Our work follows the traditional line of the Revised Shapley Ames Catalogue (Sandage & Tammann 1980), the Reference Catalogue of Bright Galaxies (de Vaucouleurs & de Vaucouleurs 1964, RC1; de Vaucouleurs et al. 1995, RC3), the Uppsala General Catalogue of Galaxies (Nilson 1973) and several others (e.g., Marzke et al. 1994; Kochanek et al. 2001; see also Blanton et al. 2005; Driver et al. 2006, which carried out rudimentary visual classifications). The size of our sample is moderate, but it is based on accurate photometric criteria to define the basic catalogue and provides a photometrically homogeneous sample that can be used for a variety of galaxy studies. We have endeavoured to alleviate subjectivity of visual classification by taking a mean of three independent classifiers.

This catalogue also allows us to verify the quality of the SDSS photometric catalogue

at the bright end. Definite photometric criteria are applied to produce a galaxy sample that is to be targeted for spectroscopic observations (Strauss et al. 2002). The problem is that we are not able to produce a genuine galaxy catalogue with simple numerical criteria. The catalogue obtained may thus contain objects that are not genuine galaxies, such as double stars, stars with somewhat deformed images, ghosts, satellite images and ‘shredded’ objects (caused by failures in deblending of large bright galaxies). On the contrary, an application of stricter criteria would miss many true galaxies, so that a compromise is needed. We visually inspect all objects that are selected with a rather loose criterion for extended objects, which permits quantification of the contamination and completeness of the photometric catalogue produced by the SDSS target selection on the bright end.

We also give a subsidiary catalogue of $r'_P \leq 15.9$ galaxies that were contained in the Early Data Release (EDR: Stoughton et al. 2002), since a number of scientific publications (Nakamura et al. 2003; Ohama 2003 (TBC:2002?); Fukugita et al. 2004; Ball et al. 2004; Nakamura et al. 2004; Yamauchi et al. 2005; Tasca & White 2005) have used this earlier version of morphologically classified galaxy catalogue. Identification of all objects in both catalogues is also given. We note that the revision in the estimate of morphological type is small, if any, for individual galaxies and the results given in the earlier papers will change little with the use of the present catalogue.

We refer the reader to the other publications for detailed descriptions of the SDSS related to our study: Gunn et al (2006) for the telescope, Gunn et al. (1998) for the photometric camera, Fukugita et al. (1996) for the photometric system, Hogg et al. (2001) and Smith et al. (2002) for external photometric calibrations, and Pier et al. (2003) for astrometric calibrations. We also refer to Abazajian et al. (2003; 2004) and Adelman-McCarthy et al. (2006) for other data releases from the SDSS, which discuss the successive improvement of the pipelines used to derive the basic catalogues.

2. Procedures

Our rectangular region is defined by $145^\circ < \alpha_{J2000} < 236^\circ$ and $-1^\circ.26 < \delta_{J2000} < 1^\circ.26$, covering an area of 230 deg^2 . This area fully encompasses SDSS survey stripe 10 but the region of primary observations that takes account of overlaps between stripes is somewhat rounded towards its corners. So we supplement the missed part from neighbouring stripes (stripes 9 and 11) to make the area strictly rectangular in celestial coordinates. We take

photometry from DR3, and select all extended objects¹ that are brighter than Petrosian magnitude $r_P = 16$ (see EDR and Strauss et al. 2002 for the precise definition) after the Galactic extinction correction (Schlegel et al. 1998). There are 2658 such objects in the DR3 catalogue that are produced from Version 5.4 of the photometric pipeline.

We note that there are some gaps (0.03 deg^2 altogether) within the region that concerns us. There are five fields (13.5×9.0) for which the photometric pipeline did not process the data (the actual gap is somewhat smaller due to overlaps with adjacent fields). This happens when the field contains very bright galaxies or stars with conspicuous spikes, and the completion of deblending required more time than the pipeline limit. Any galaxies located in these fields are not included in our sample.

All objects are visually inspected by three classifiers (MF, ON, SO) independently. This sample is contaminated by non-galactic objects. Our initial sample of 2658 objects includes a number of sources that are not galaxies (stars, satellite trails, optical defects) as well as multiple entries for a single object (primarily due to deblending failures). Removal of these objects produces a final sample of 2253 galaxies.

Morphological classification is carried out in reference to *The Hubble Atlas of Galaxies* by Sandage (1961; Hubble Atlas hereafter) by three classifiers using the SAOimage viewer. We use the monochromatic g band image, which is similar to the commonly-used B band image for classification, and is sensitive to HII regions and arm structures. It is important to inspect images with both linear and logarithmic scales in the viewer with varying contrast levels. This occasionally produces a systematic difference from classifications based on photographic materials. We intentionally avoid using colour information so that morphology is solely determined by the appearance, as has been done traditionally. This allows us to consider the correlation between morphology and colours in an unbiased way.

We consider classification into 7 classes, $T = 0$ (E), 1 (S0), 2(Sa), 3(Sb), 4(Sc), 5(Sd) and 6(Im), allowing for half-integer classes. We do not adopt more detailed classes such as those defined in RC3 (which has 16 classes in T), since our experience with the SDSS data (comparing results from the three classifiers) is that a finer division is unwarranted. The Hubble Atlas does not define Sd and Sdm. We assign the latest of the Sc galaxies in the Hubble Atlas as Sd–Sdm so that our classification scheme matches with that in RC3. Irr I of the Hubble Atlas is denoted as Im in this paper, also in agreement with RC3. We assign $T = -1$ when we are unable to classify a galaxy into a conventional Hubble type. We indicate

¹Technically, the selection is made using flag `type=3` (galaxy), not `saturated`, and not `satur_center` for all colour bands. Objects that are flagged as `type=3`, and not `satur_center` but flagged as `saturated` are visually inspected and included into the catalog when appropriate.

by a symbol “p” when some peculiarity is noted in a galaxy (such as somewhat disturbed shapes, rings, dust lanes etc. as in the Hubble Atlas) even though it can be classified into a regular, $T \neq -1$, Hubble type. The relation between our T and $T(\text{RC3})$ is shown in Table 1. We note slight biases in our classification towards integer T . We are not concerned with whether galaxies have bars or not.

During the classification we noticed that not all galaxies fell nicely into the Hubble sequence, but whenever reasonable we classified a galaxy into the $T = 0$ to 6 scale. This leads to a number of cases where the appearance of the galaxy may not match well with the appearance of the Hubble Atlas prototype, but we view this as preferable to a catalogue containing a large number of unclassifiable ($T = -1$) objects. Our catalogue contains 33 galaxies with $T = -1$.

We noted that some galaxies, notably among those with $T = -1$, show a common feature, characterised by a high surface brightness and a smooth light distribution, but their appearance is definitely not that of E or S0 galaxies. These objects frequently have more irregular shapes than early-type galaxies, but the light distribution is too smooth and/or surface brightness too high to be classified as Im. They appear to be reminiscent of Irr II in the Hubble Atlas or ‘amorphous’ galaxies introduced by Sandage and Brucato (1979), who characterised them as ‘not E, S0, or any type of spiral no matter how peculiar, but rather have an amorphous appearance to the unresolved light’. Gallagher & Hunter (1987) used the term amorphous to represent ‘all galaxies with E/S0-like morphologies whose other global properties resemble irregular galaxies.’ These definitions, however, are not quite clear. These galaxies tend to show a red colour. We confirmed that most of the galaxies of this type in our sample show red colours, although we did not use the colour information when we classified galaxies. We indicate by “am” when we encounter those galaxies, whether they are left unclassified or classified into regular types (see a figure given at the end of Section 3).

If the SDSS photometric pipeline determines that an image is actually composed of more than one component, the ‘parent’ image is deblended into ‘child’ images (Lupton 2006). The child images may be further deblended if they are judged to be formed of more than one component. When confronted with a large, complex surface brightness pattern, the deblender ‘shreds’ a bright extended galaxy into a multitude of components, which can obviously affect the morphology of the galaxy (and also photometric measurements). (An extreme example is the separation of a nucleus, which may look as S0, from a spiral galaxy.) For this reason it is important to inspect both parent and child images for all objects to ensure correct classifications.

Each classifier independently carries out the classification of each galaxy at least twice.

The results are then compared, and when the results for an individual galaxy differ by more than 1.5 units in T , all classifiers reinspect the galaxy in question and make a final, independent assessment. The adopted morphological classification is the mean of the measurements of the three classifiers.

The panels in Figure 1 display the correlation in T among the three classifiers. The dispersion is 0.4, or ≈ 1 in the RC3 T scale. This is probably as good as can be expected for visual classification; for example, $\delta T(\text{RC3}) = 1.8$ in Lahav et al. (1995), a study that used photographic prints.

The final SDSS sample contains 218 galaxies that have assigned $T(\text{RC3})$ in the RC3 catalogue. Figure 2 shows the correlation of $T(\text{RC3})$ versus those from our classification for those common galaxies. The correlation is generally good; however, there is a systematic difference in the classifications in that S0/a to Sa(Sab) galaxies in RC3 are classified somewhat later to Sa to Sb (occasionally to Sc) in our catalogue. On the other hand, our E and S0 galaxy samples do not contain any galaxies that are classified as S0/a or later in RC3. We suspect the main reason of the discrepancy to be that our classification is based on high dynamic range and high contrast CCD images, which allows detection of arm structure and detailed texture that could not be apparent in a single photometric image. This will drive our classification of disc galaxies towards later types, compared to those in the RC3 catalogues.

The quality of the photometry is also examined by visual inspection of images, to check whether the SDSS atlas image contains the entire image of the galaxy. If these data contain extra objects or parts of the galaxy are erroneously removed by the deblender, flags are attached. The position of spectroscopic fibre, which has a diameter of $3''$, is also inspected. When the fibre is not centred on the nucleus, but is assigned to a region of the galaxy (e.g., a bright HII region), the spectroscopic information is accepted but flagged.

3. Catalogue

Table 2 presents our final catalogue from DR3 ($r_P \leq 16$) in the order of right ascension, but only the top 20 lines are shown in the printed version of the paper. The entire catalogue is available in an electronically readable format. The catalogue contains 15 columns with the following information:

- Column 1: catalogue number;
- Column 2: photometric identification number in DR3. The numbers mean run (ob-

ervation) – rerun (photometric data reduction) – camcol (camera column) – field – object id (see DR3 for details);

- Column 3: right ascension (J2000), in decimal degrees;
- Column 4: declination (J2000), in decimal degrees;
- Column 5: photometric identification number in EDR (see explanation for Column 2);
- Column 6: I_{sample} flag for catalogue inclusions: [3] in both DR3 ($r_P \leq 16$) and EDR ($r_P \leq 15.9$); [2] only in DR3 ($r_P \leq 16$);
- Column 7: I_{target} flag for spectroscopic target selection: [0] not targeted; [1] targeted but not observed; [2] observed; [2:] fibre positioned off-nucleus, but on some other part of the object carrying the specified photometric identification;
- Column 8: morphological index T : the mean of three classifiers rounded to the nearest integer or half-integer;
- Column 9: standard deviation of morphological indices among three classifiers;
- Column 10: I_{ph} photometry quality: [0] good photometry (typical error expected to be smaller than approximately 0.1 mag based on visual estimates); [1] photometry is accurate if one uses the magnitude given to the parent image; [2] some errors, say 0.3 mag (with visual estimates), is suspected in photometry; [3] poor photometry. (Note that these flags are somewhat subjective.) Flags 2 and 3 are occasionally appended by p or c, which means that more accurate magnitudes may easily be obtained by applying aperture photometry centred on the designated object using parent or child atlas image frames, respectively.
- Column 11: Petrosian r magnitude (of the child image) after correcting for Galactic extinction;
- Column 12: spectroscopic identification number: spectroscopic plate number– mjd –fibre number;
- Column 13: heliocentric redshift;
- Column 14: confidence level of redshift measurements;
- Column 15: remarks: ‘p’ stands for peculiar, and this flag is given only when galaxies are classified into normal types. ‘am’ is given to galaxies with an amorphous appearance. ‘int’ stands for interacting, and ‘d-nucl’ for double nuclei within a single galaxy.

‘double’ and ‘multiple’ stand for more than one galaxy in the child field, while interactions among them are not apparent. The PGC number is provided when the galaxy is identified with that listed in RC3.

In the bottom of Table 2 we append a similar catalogue for 22 objects that are included only in our EDR sample ($r_P \leq 15.9$). All of the galaxies have Galactic-extinction corrected $r_P > 16$ in DR3; This change from the EDR measurement is due to reprocessing the EDR data with the improved DR3 photometric pipeline. Flag [1] is assigned to Column 6, ‘flag for catalogue inclusions’. We carried out reclassifications for the EDR sample, but the change compared to the earlier catalogue is insignificant.

Figures 3–7 display examples of *gri* colour synthetic images of galaxies (20 each) that are classified as $T = 0 - 4$, taken from Catalog Archive Server (CAS). Figure 8 shows images for $T = 5$ (8 galaxies in the top) and $T = 6$ (12 galaxies in the bottom). Note that detailed textures are not quite visible on these pictures and the contrast is not always well represented, so that these printed images are not always appropriate for the purpose of classification. Figure 9 shows 12 galaxies, which we classified as interacting; the four galaxies in the bottom row have double (multiple) nuclei. Figure 10 shows 16 galaxies to which we give amorphous (“am”) flags. The size of pictures are all $1' \times 1'$.

4. Verification of the photometric catalogue of DR3

We have adopted a set of inclusive selection criteria so that few galaxies are missed in our initial sample. This selection is substantially looser than that adopted in the operational spectroscopic target selection for galaxies (Strauss et al. 2002).

Among 2658 extended objects in our sample, 2253 are unique galaxies. There are 27 examples of galaxies that are included two or more times in the initial list; this primarily arises from deblending difficulties. Also included in our original set are 211 stars (approximately 80% of which are double stars) and 167 spurious objects, such as satellite trails, diffraction spikes of bright stars, ghosts, failures of deblending or of removal of bright stars that saturate the CCD, and empty fields with no designated object (which happen typically when imaging of the same fields with other colour bands was hit by satellite trails). Nearly all stars (206 out of 211) can be rejected if one imposes the condition $g(\text{PSF}) - g(\text{model}) > 0.5$ for the selection of galaxies, which is tighter than the one used in target selection, $r(\text{PSF}) - r(\text{model}) > 0.3$. The former condition rejects six true galaxies (one among them looks like an AGN); 61 spurious objects, however, escape the rejection and contaminate the galaxy sample.

Among the 2253 galaxies, 2213 (98.2 %) are chosen by SDSS target selection, and 1866

(82.8% of the entire galaxy sample) are actually spectroscopically observed². The completeness of the spectroscopic observation in our sample is essentially uniform from early- to late-types within Poissonian error. One reason for missing spectroscopy is the fibre separation constraint (fibres on a given plate must be separated by at least $55''$, Blanton et al. 2003b). In cases where a galaxy and a quasar candidate conflict, the fibre is assigned to the latter. We found a few patches for which spectroscopic observations were not carried out for unknown reasons. We also found that 168 more targets are set by target selection on non-galactic objects, of which 18 are observed³

The survey samples are summarised in Table 3. The spectroscopic sample is quite clean even for bright galaxies of our sample, but with a completeness of 83%. We wish to inject a note of caution to the use of SDSS photometric galaxy catalogues. The target-selection algorithm of Strauss et al. yields a sample of galaxies with good completeness, only 2% of galaxies missed, but suffers a 7% contamination by stars and spurious objects.

In order to examine the statistical completeness, we show in Figure 11 the number of galaxies as a function of r magnitude. The solid line shows $N \sim 10^{0.6r}$ expected for Euclidean geometry. The data indicate that the galaxy number count deviates little from this line from 10 to 16 mag. A slight excess at bright magnitudes is consistent with the Poisson statistics. This implies that we have not missed too many galaxies even in the bright end of the sample at 10–10.5 mag. The spectroscopic sample is indicated by shading, which shows that the spectroscopic completeness stays nearly constant for $r > 12.5$. The thick shades indicates galaxies that carry a flag for photometric errors, which increases towards brighter magnitudes, from 5% at $r = 15.5$ to 20% at $r = 13$. The number count for each morphological type is shown in Figure 12. All curves are consistent with $N \sim 10^{0.6r}$ up to statistical errors, indicating homogeneity in morphological compositions, and therefore morphological fractions change little as a function of magnitude to $r = 16$. We note, however, that the region considered has some over-density at $z \sim 0.8$ where more early-type galaxies are included (see Figure 2 of Nakamura et al.). This may cause a slight deviation from the smooth $10^{0.6r}$ growth.

An additional test is carried out for the completeness by comparing galaxies in our

²Note that stripe 10 was observed in early days of the SDSS observation, when the tuning of spectroscopic observations was still immature. We suspect a higher rate of spectroscopic observations for stripes observed in later times.

³We suspect that these rather large numbers are likely due to deblending errors of the early immature version of photometric pipeline used for spectroscopic target selection, since spectroscopic observations are carried out in early stages of SDSS operations for the region that concerns us in this paper.

sample with those in RC3 and Updated Zwicky Catalogues (Falco et al. 1999). The RC3 contains 269 galaxies in our survey area; 15 of these are not in our catalogue. Nine of the 15 are too faint to us ($r > 16$), and 2 are omitted because they lie too close to the edge of our area. Three (PGC33550, PGC39695; PGC39705) are in the field for which the SDSS photometric pipeline could not process the frame due to the presence of the excessively bright stars (for the first two) or the bright galaxy itself (PG33550, $B_T = 9.8$). The one (PGC53499=NGC5792) is a bright galaxy but lies too close to a very bright star. In summary, only 4 of 258 RC3 galaxies that should have been included in our catalogue were missed.

A similar result was obtained in a comparison of the 394 updated Zwicky Catalogue objects in our survey area; 14 of these objects were missed. One Zwicky galaxy (one of a pair of interacting galaxies) was shredded by the deblender into components that all had $r > 16$, and hence dropped from our catalogue. In total, four bright Zwicky galaxies (there are three in common to those we found for the case of RC3) that should have been in our catalogue were missed by the SDSS photometric pipeline.

From these tests we conclude that galaxies are well sampled to as bright as 10 mag, unless they are accidentally located close to very bright stars. The most important cause of missing bright galaxies is failures of deblending in the presence of very bright stars or galaxies themselves; we missed the fraction of the region, $\approx 1.3 \times 10^{-4}$. We expect that the incompleteness will become an important issue for $r \lesssim 10$. A comparison with the RC3 catalogue (which includes all Zwicky galaxies) shows that incompleteness for low-surface brightness galaxies is no more than that in RC3.

5. Statistics

Figure 13 shows histograms of the morphological type distribution of galaxies for both photometric and spectroscopic samples. We use only seven classes, grouping half those classified into half-integer T into each adjoining integer bins. The fractional morphological composition of our catalogue breaks down to E: E/S0–S0: S0a–Sab: Sb–Sc: Scd–Sdm: Im = 0.14: 0.26: 0.25: 0.28: 0.038: 0.014. A B band study summarised by Fukugita, Hogan & Peebles (1998) gives a relative frequency of E: S0: Sab: Sbc: Scd: Im = 0.11: 0.21: 0.28: 0.29: 0.045: 0.061. A somewhat higher fraction of early type galaxies in our sample is ascribed to our galaxy selection in the r magnitude, which will select a larger fraction of early-type galaxies than would be present in a volume-limited sample. Our small fraction of Im galaxies arises from the intrinsic small luminosity of these sources that makes the sampling volume small. These issues are discussed in Nakamura et al. (2003), where the

morphologically classified luminosity function is derived.

We identified 25 galaxies which are interacting, and an additional six that display features that suggest interacting. Of this set of 31, 16 have such disturbed morphologies that they are assigned $T = -1$ (unclassified). In our galaxy sample 12 galaxies have double (or multiple) nuclei, and four of these are also counted as “interacting” and 1 suspected interacting. Adding double-nucleus galaxies, we arrive at 33–38 interacting galaxies in our catalogue, i.e., the rate of interacting galaxies in a nearby magnitude-limited galaxy sample is 1.5-1.7%.

The mean colours of galaxies after K corrections (Blanton et al. 2003a) are given in Table 4. We have rejected galaxies for which poor photometry is suspected ($I_{\text{ph}} \geq 2$). This information supersedes the mean colours given in Shimasaku et al. (2001)⁴. The colours, except for $i - z$, form monotonic sequences from red to blue with increasing T , including half integer types that are not shown in this table. The scatter of colours among different galaxies at given T is larger than the difference between the mean colours of the neighbouring types. For example, the mean colours of E galaxies for $u - g$, $g - r$ and $r - i$ are within one standard deviation of those of Sa galaxies. The $i - z$ colours stay essentially constant from E to Sab. For later types, some bluing trend is present in $i - z$, but the scatter widens and is larger than the variation. The mean colours of E galaxies are $u - g = 1.73 \pm 0.18$ (1.99), $g - r = 0.77 \pm 0.04$ (0.77), $r - i = 0.39 \pm 0.03$ (0.43), $i - z = 0.18 \pm 0.04$ (0.36), where the numbers in parentheses are the spectrosynthetic calculation of Fukugita et al. (1995). There is a significant disagreement in the reddest colours, as was noted by Shimasaku et al. (2001).

This work was supported in Japan by Grant-in-Aid of the Ministry of Education. MF received support from the Monell Foundation at the Institute for Advanced Study.

Funding for the SDSS and SDSS-II has been provided by the Alfred P. Sloan Foundation, the Participating Institutions, the National Science Foundation, the U.S. Department of Energy, the National Aeronautics and Space Administration, the Japanese Monbukagakusho, the Max Planck Society, and the Higher Education Funding Council for England. The SDSS Web Site is <http://www.sdss.org/>. The SDSS is managed by the Astrophysical Research Consortium for the Participating Institutions. The Participating Institutions are the

⁴Shimasaku et al. (2001) do not include K corrections due to a lack of redshift at that time. Although the galaxies are all at low redshift, the absence of K corrections make galaxies, especially those of early types, redder by a non-negligible amount. Without the K correction the colours quoted below in this paragraph will be 1.85, 0.89, 0.41 and 0.28 for the sample used in the present paper.

American Museum of Natural History, Astrophysical Institute Potsdam, University of Basel, Cambridge University, Case Western Reserve University, University of Chicago, Drexel University, Fermilab, the Institute for Advanced Study, the Japan Participation Group, Johns Hopkins University, the Joint Institute for Nuclear Astrophysics, the Kavli Institute for Particle Astrophysics and Cosmology, the Korean Scientist Group, the Chinese Academy of Sciences (LAMOST), Los Alamos National Laboratory, the Max-Planck-Institute for Astronomy (MPIA), the Max-Planck-Institute for Astrophysics (MPA), New Mexico State University, Ohio State University, University of Pittsburgh, University of Portsmouth, Princeton University, the United States Naval Observatory, and the University of Washington.

REFERENCES

- Adelman-McCarthy, J. K., et al. 2006, *ApJS*, 162, 38
- Abazajian, K., et al. 2003, *AJ*, 126, 2081
- Abazajian, K., et al. 2004, *AJ*, 128, 502
- Abazajian, K., et al. 2005, *AJ*, 129, 1755
- Ball, N. M., Loveday, J., Fukugita, M., Nakamura, O., Okamura, S., Brinkmann, J., & Brunner, R. J. 2004, *MNRAS*, 348, 1038
- Blanton, M. R., et al. 2003a, *AJ*, 125, 2348
- Blanton, M. R., Lin, H., Lupton, R. H., Maley, F. M., Young, N., Zehavi, I., & Loveday, J. 2003b, *AJ*, 125, 2276
- Blanton, M. R., et al. 2005, *AJ*, 129, 2562
- Driver, S. P., et al. 2006, *arXiv:astro-ph/0602240*
- Falco, E. E., et al. 1999, *PASP*, 111, 438
- Fukugita, M., Shimasaku, K., & Ichikawa, T. 1995, *PASP*, 107, 945
- Fukugita, M., Ichikawa, T., Gunn, J. E., Doi, M., Shimasaku, K., & Schneider, D. P. 1996, *AJ*, 111, 1748
- Fukugita, M., Hogan, C. J., & Peebles, P. J. E. 1998, *ApJ*, 503, 518
- Fukugita, M., Nakamura, O., Turner, E. L., Helmboldt, J., & Nichol, R. C. 2004, *ApJ*, 601, L127

- Gallagher, J. S., & Hunter, D. A. 1987, *AJ*, 94, 43
- Gunn, J. E., et al. 1998, *AJ*, 116, 3040
- Gunn, J. E., et al. 2006, *astro-ph/0602326*
- Hogg, D. W., Finkbeiner, D. P., Schlegel, D. J., & Gunn, J. E. 2001, *AJ*, 122, 2129
- Kochanek, C. S., et al. 2001, *ApJ*, 560, 566
- Lahav, O., et al. 1995, *Science*, 267, 859
- Lupton, R. H. 2006, *AJ*, submitted
- Marzke, R. O., Geller, M. J., Huchra, J. P., & Corwin, H. G. 1994, *AJ*, 108, 437
- Nakamura, O., Fukugita, M., Yasuda, N., Loveday, J., Brinkmann, J., Schneider, D. P., Shimasaku, K., & SubbaRao, M. 2003, *AJ*, 125, 1682
- Nakamura, O., Fukugita, M., Brinkmann, J., & Schneider, D. P. 2004, *AJ*, 127, 2511
- Nilson, P. 1973, *Uppsala General Catalogue of Galaxies* (Uppsala: Astronomiska Observatorium, 1973)
- Ohama, N. 2003, Master thesis, University of Tokyo
- Pier, J. R., Munn, J. A., Hindsley, R. B., Hennessy, G. S., Kent, S. M., Lupton, R. H., & Ivezić, Ž. 2003, *AJ*, 125, 1559
- Sandage, A. 1961, *The Hubble Atlas of Galaxies*, Washington: Carnegie Institution, 1961,
- Sandage, A., & Brucato, R. 1979, *AJ*, 84, 472
- Sandage, A., & Tammann, G. A. 1980, *A Revised Shapley-Ames Catalog of Bright Galaxies*, Washington: Carnegie Institution, 1980
- Schlegel, D. J., Finkbeiner, D. P., & Davis, M. 1998, *ApJ*, 500, 525
- Shimasaku, K., et al. 2001, *AJ*, 122, 1238
- Smith, J. A., et al. 2002, *AJ*, 123, 2121
- Stoughton, C., et al. 2002, *AJ*, 123, 485
- Strauss, M. A., et al. 2002, *AJ*, 124, 1810

- Tasca, L. A. M., & White, S. D. M. 2005, ArXiv Astrophysics e-prints, arXiv:astro-ph/0507249
- de Vaucouleurs, G., & de Vaucouleurs, A. 1964, Reference Catalogue of Bright Galaxies (Austin: University of Texas Press) (RC1)
- de Vaucouleurs, G., de Vaucouleurs, A., Corwin, H. G., Buta, R. J., Paturel, G., & Fouqué, P. 1995, Third Reference Catalogue of Bright Galaxies (New York: Springer-Verlag) (RC3)
- Yamauchi, C., et al. 2005, AJ, 130, 1545
- York, D. G., et al. 2000, AJ, 120, 1579

Table 1. Morphological index T

Hubble type	E	S0	Sa	Sb	Sc	Sd	Im	unclass.
$T(\text{ours})$	0	1	2	3	4	5	6	–1
$T(\text{RC3})$	–6 to –4	–3 to –1	1	3	5	7 to 8	10	

Table 2. Catalogue of Morphologically Classified Galaxies

ID	DR3 photo-ID	$\alpha_{J2000}(^{\circ})$	$\delta_{J2000}(^{\circ})$	EDR photo-ID	I_{sample}	I_{target}	T	$\sigma(T)$	I_{ph}	r_P	Spectro-ID	z	CL(z)	remarks
1	0756-44-6-0195-0158	145.00014	1.10623	-	2	2	0.5	0.4	0	15.64	477-52026-100	0.0605	0.999	
2	0756-44-4-0195-0158	145.04410	0.22011	-	2	2	3.0	0.0	0	15.49	476-52314-587	0.0621	0.998	
3	0756-44-4-0195-0165	145.04752	0.23774	-	2	2	1.0	0.4	0	15.25	476-52314-585	0.0622	0.999	
4	0756-44-5-0195-0208	145.06132	0.70924	-	2	2	3.5	0.5	0	15.61	477-52026-98	0.0260	0.958	
5	0756-44-4-0196-0172	145.22040	0.41082	756-4-8-0196-0174	3	2	3.5	0.6	0	15.89	266-51630-350	0.0982	1.000	
6	1239-40-1-0167-0166	145.37412	-1.24928	752-1-8-0012-0078	3	1	0.0	0.4	0	14.89	-	0.000	0.000	
7	0756-44-4-0198-0055	145.51373	0.33644	-	2	1	4.0	0.0	2p	11.77	-	0.000	0.000	PGC2773
8	1239-40-2-0169-0142	145.64788	-0.77173	752-2-8-0014-0175	3	2	3.0	0.8	0	15.75	266-51630-215	0.0218	0.992	
9	0756-44-1-0199-0259	145.68110	-0.86723	756-1-8-0199-0148	3	2	2.0	0.5	0	15.60	266-51630-207	0.0676	0.999	
10	1239-40-2-0170-0139	145.75971	-0.81389	-	2	2	2.5	0.5	0	15.96	266-51630-216	0.0676	0.946	
11	1239-40-1-0170-0201	145.76792	-1.07472	752-1-8-0015-0167	3	1	3.5	0.5	0	15.84	-	0.000	0.000	
12	0756-44-4-0200-0098	145.80018	0.41417	756-4-8-0200-0158	3	2	4.0	0.4	0	14.18	266-51630-430	0.0252	0.996	PGC27803
13	0756-44-5-0200-0211	145.84750	0.67573	0756-5-8-0200-0131	3	2	2.5	0.5	0	15.87	266-51630-422	0.0266	1.000	
14	0756-44-6-0200-0100	145.85049	1.20353	756-6-8-0200-0063	3	2	1.5	0.5	0	15.60	480-51989-272	0.0618	1.000	
15	1239-40-4-0170-0202	145.87328	0.05683	752-4-8-0015-0058	3	1	1.0	0.4	0	15.88	-	0.000	0.000	
16	0756-44-2-0201-0130	145.87445	-0.60876	756-2-8-0201-0156	3	2	4.0	0.0	0	15.89	266-51630-138	0.0715	0.999	
17	0756-44-6-0201-0022	145.89254	1.11773	-	2	2	-1.0	0.0	0	15.93	480-51989-266	0.0512	0.986	int, am
18	1239-40-5-0171-0179	145.94781	0.46530	752-5-8-0016-0090	3	2	1.0	0.8	0	15.17	266-51630-467	0.0304	0.997	
19	1239-40-2-0171-0091	146.00780	-0.64227	752-2-8-0016-0100	3	2	-1.0	0.0	2p	15.89	266-51630-100	0.0051	0.938	
20	0756-44-5-0202-0018	146.02092	0.73355	756-5-8-0202-0009	3	2	0.5	0.6	0	14.10	266-51630-461	0.0362	0.999	

Table 3. Numbers of objects

Galaxy sample	Galaxy	Double counted	Star/spurious	Initial sample
Photometric sample.....	2253	27	378	2658
Targetted spectroscopic sample.....	2213	20	168	2401
Observed spectroscopic sample.....	1866	0	18	1884

Table 4. Statistical properties of galaxies

Hubble type	E	S0	Sa	Sb	Sc	Sd	Im
Number	265	255	139	188	166	9	18
$u - g$	1.73 ± 0.18	1.65 ± 0.21	1.50 ± 0.29	1.33 ± 0.28	1.35 ± 0.26	1.18 ± 0.10	1.15 ± 0.34
$g - r$	0.77 ± 0.04	0.74 ± 0.07	0.68 ± 0.10	0.60 ± 0.13	0.54 ± 0.10	0.47 ± 0.09	0.36 ± 0.13
$r - i$	0.39 ± 0.03	0.38 ± 0.04	0.35 ± 0.05	0.31 ± 0.09	0.26 ± 0.08	0.16 ± 0.08	0.09 ± 0.11
$i - z$	0.18 ± 0.04	0.19 ± 0.05	0.18 ± 0.07	0.15 ± 0.09	0.06 ± 0.13	0.01 ± 0.15	-0.06 ± 0.21

Note. — Those galaxies that are classified as a half-integer type are omitted from these statistics. The error stands for the dispersion.

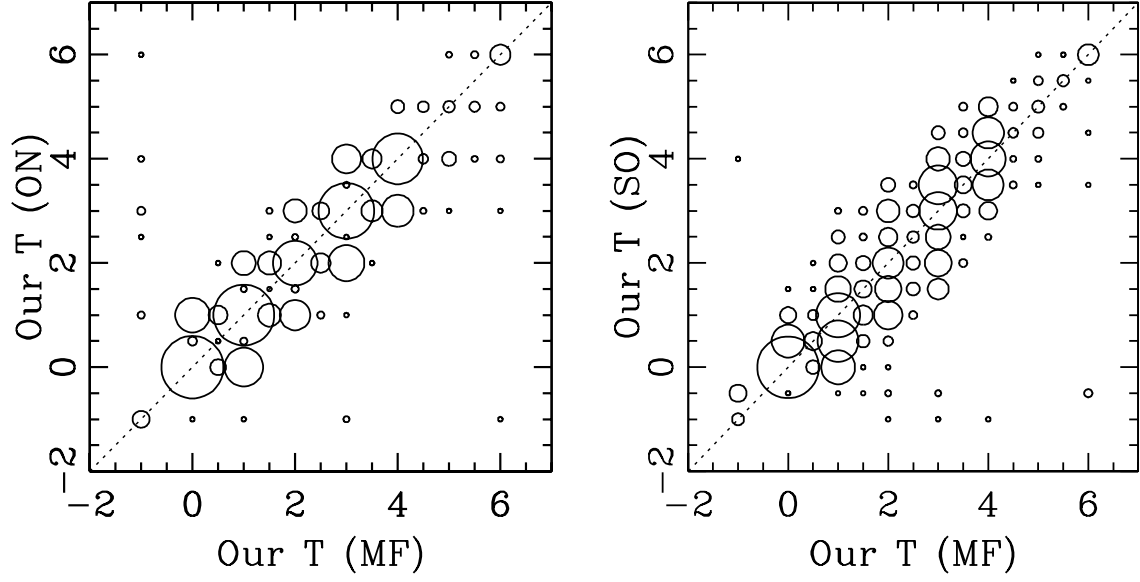


Fig. 1.— Correlation of visually inferred morphological types among three classifiers. The area of the circle represents the number of galaxies in the grid.

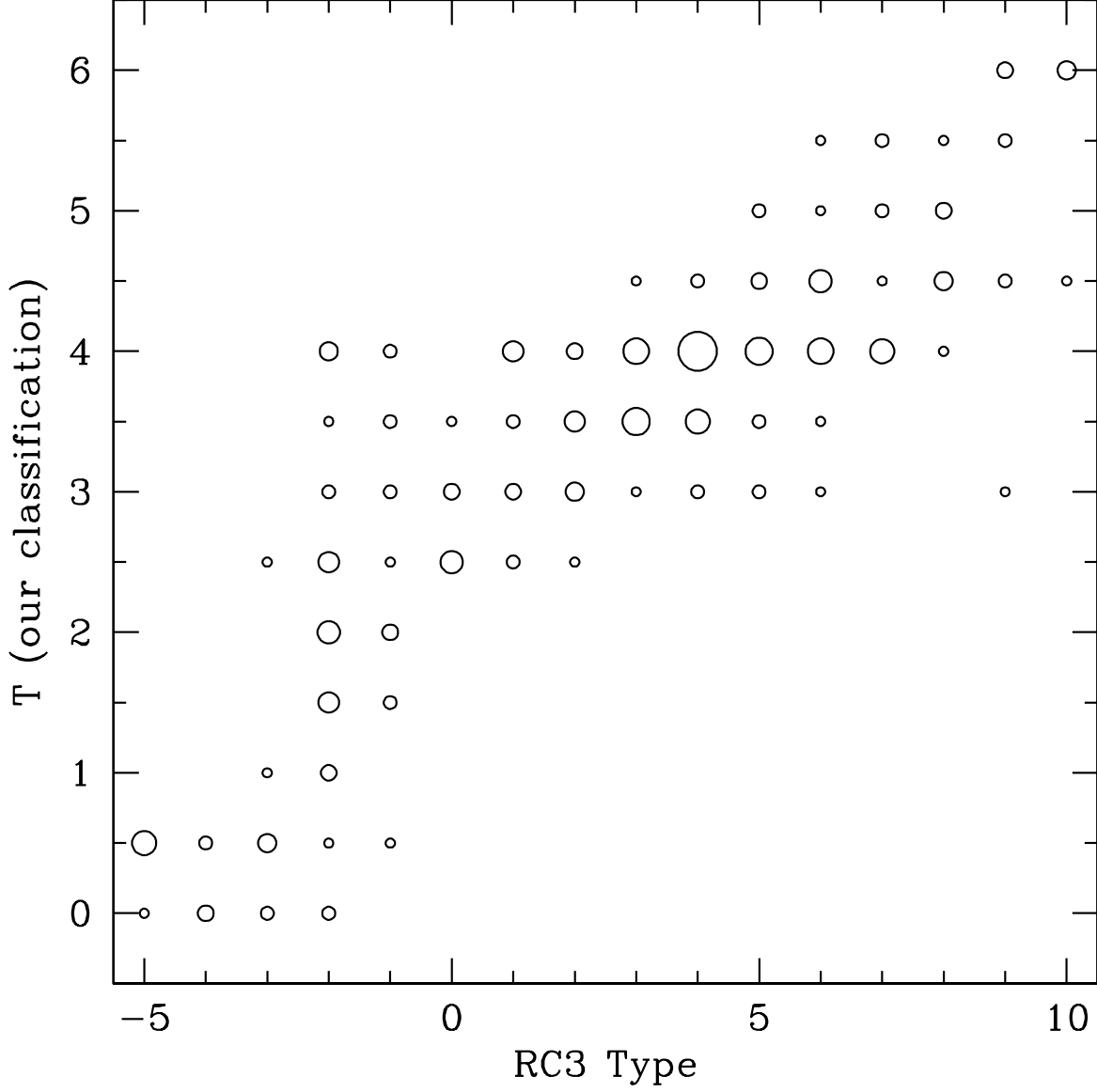


Fig. 2.— Correlation of our T with those of RC3 for 218 galaxies common to the two samples. The area of the circle represents the number of galaxies in the grid.

Fig. 3.— Sample of E ($T = 0$) galaxies with synthetic gri colour. The size is $1' \times 1'$ for all pictures.

Fig. 4.— Sample of S0 ($T = 1$) galaxies. The format is the same as for Figure 3.

Fig. 5.— Sample of Sa ($T = 2$) galaxies. The format is the same as for Figure 3.

Fig. 6.— Sample of Sb ($T = 3$) galaxies. The format is the same as for Figure 3.

Fig. 7.— Sample of Sc ($T = 4$) galaxies. The format is the same as for Figure 3.

Fig. 8.— Sample of Sd ($T = 5$) and Im ($T = 6$) galaxies. The top two rows display Sd galaxies, and the bottom three Im galaxies. The other format is the same as for Figure 3.

Fig. 9.— Sample of interacting galaxies. The 4 galaxies in the bottom row are galaxies with double nuclei. The format is the same as for Figure 3.

Fig. 10.— Sample of galaxies with “amorphous” appearance. The format is the same as for Figure 3.

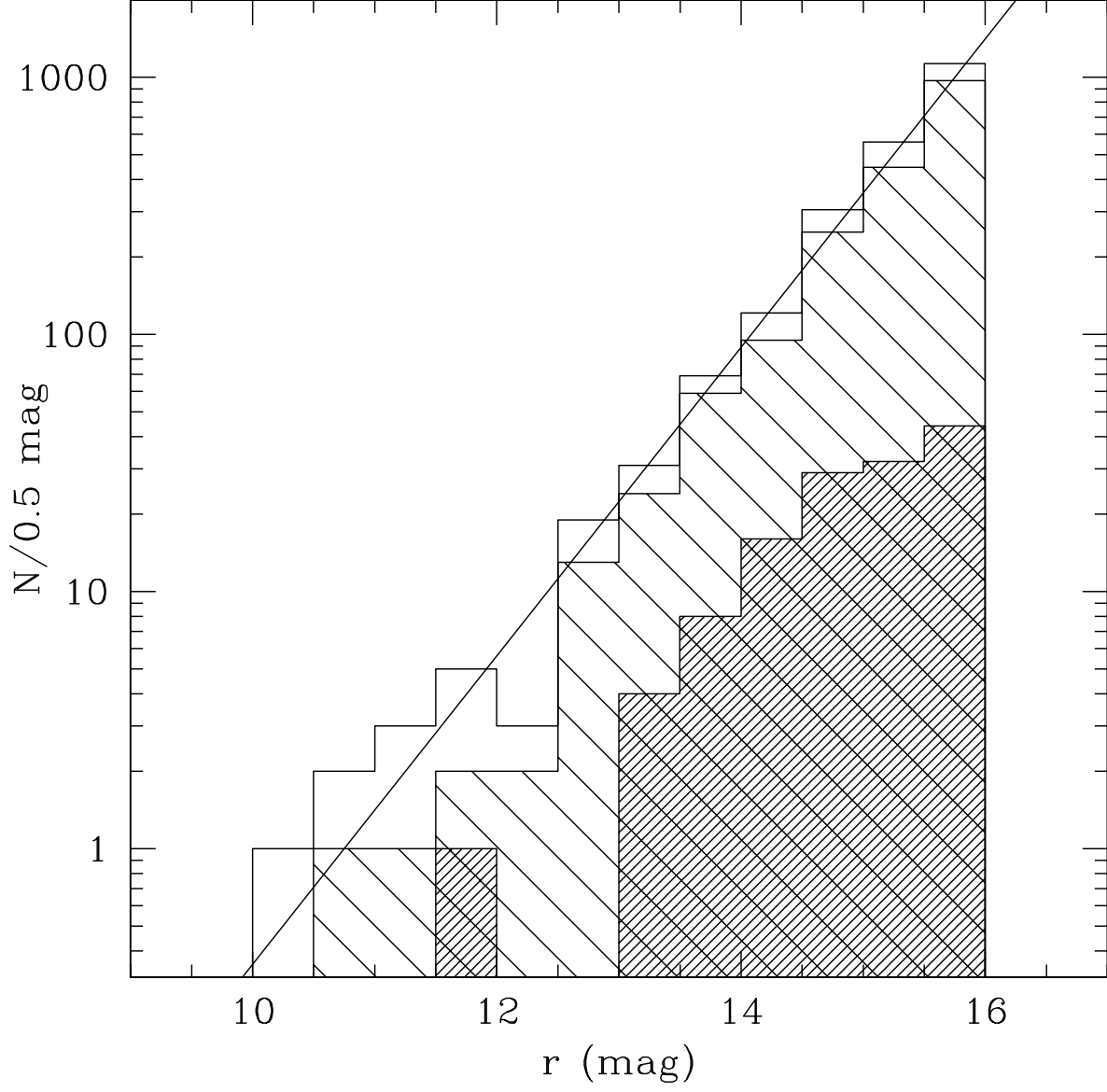


Fig. 11.— Number of galaxies in our catalogue per 0.5 mag as a function of r mag. The spectroscopic sample is shown with light shading. Galaxies that carry a flag for photometric errors are indicated by thick shading. The curve shows the Euclidean growth, $N \sim 10^{0.6r}$.

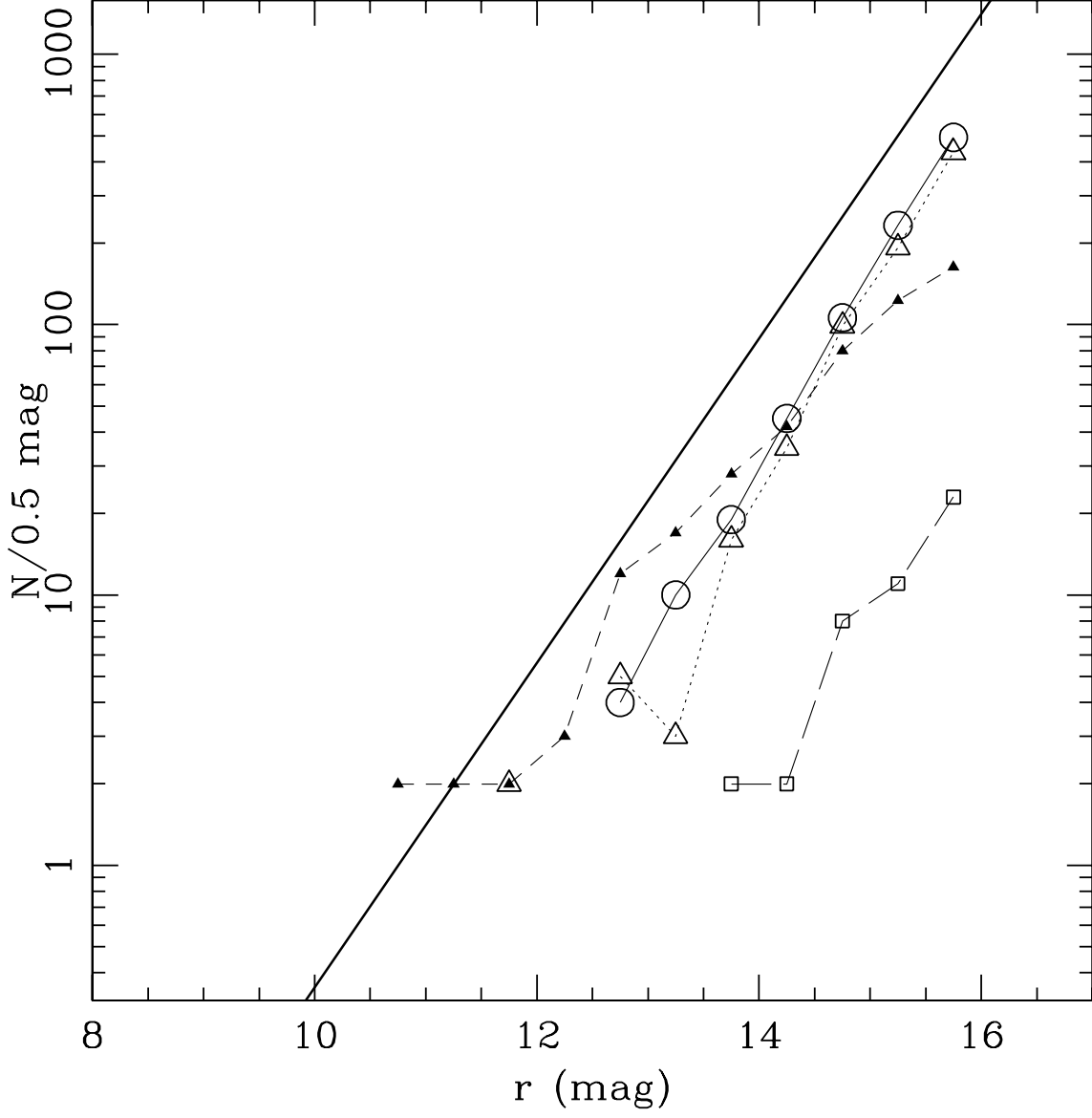


Fig. 12.— The same as Figure 11 but for each type. Points with $N \geq 2$ are plotted. Circles, open triangles, filled triangles, squares indicate $T = 0 - 1$, $1.5 - 3$, $3.5 - 5$, and $5.5 - 6$, respectively. The thick solid line denotes the line of $N \sim 10^{0.6r}$ shown in Figure 11.

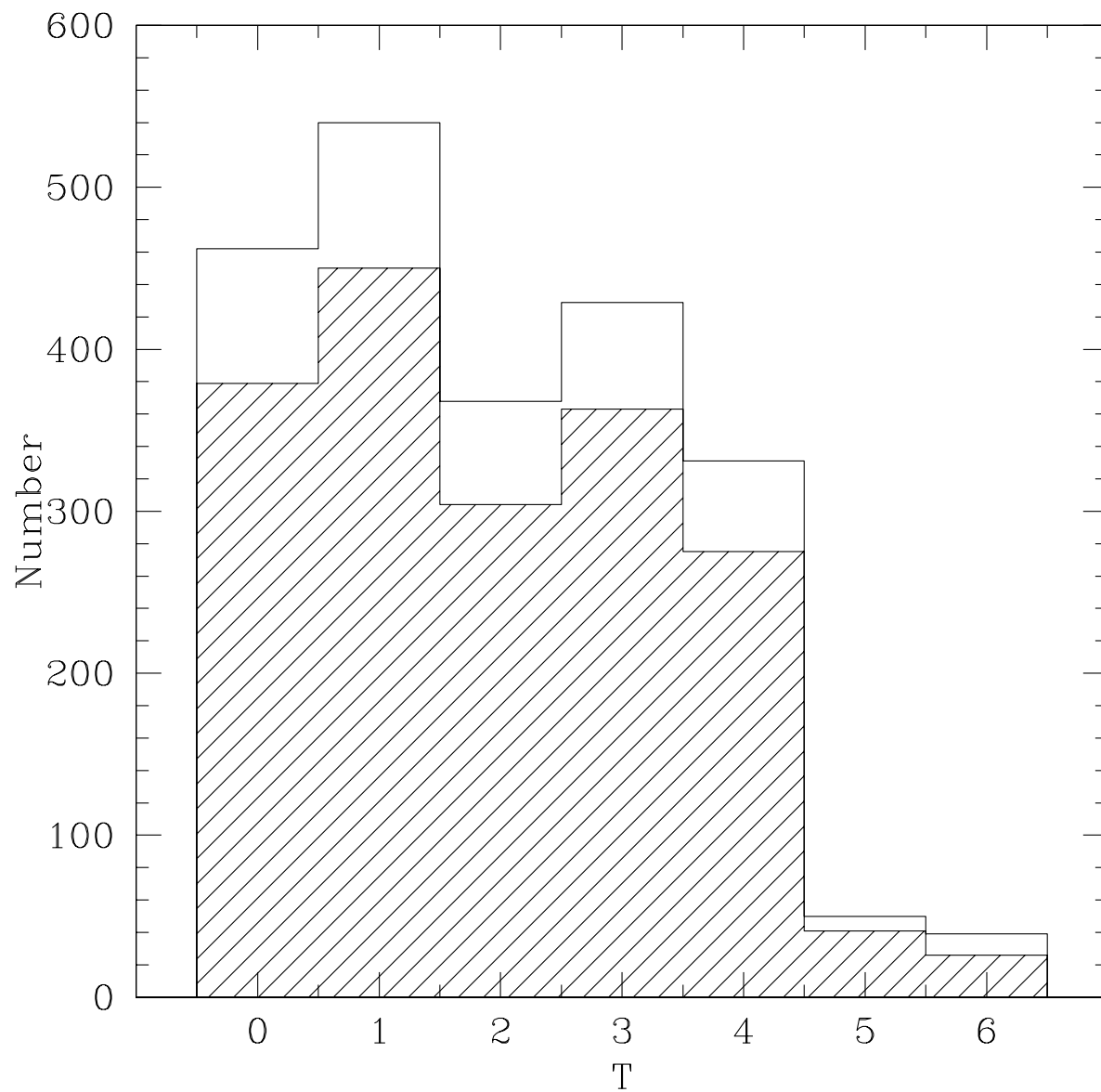


Fig. 13.— Distribution of the morphological types in the galaxy sample selected with $r \leq 16$. Galaxies with half-integer T indices are grouped into each adjoining integer bins. Shading represents the spectroscopic sample.

This figure "figure3.jpg" is available in "jpg" format from:

<http://arXiv.org/ps/0704.1743v1>

This figure "figure4.jpg" is available in "jpg" format from:

<http://arXiv.org/ps/0704.1743v1>

This figure "figure5.jpg" is available in "jpg" format from:

<http://arXiv.org/ps/0704.1743v1>

This figure "figure6.jpg" is available in "jpg" format from:

<http://arXiv.org/ps/0704.1743v1>

This figure "figure7.jpg" is available in "jpg" format from:

<http://arXiv.org/ps/0704.1743v1>

This figure "figure8.jpg" is available in "jpg" format from:

<http://arXiv.org/ps/0704.1743v1>

This figure "figure9.jpg" is available in "jpg" format from:

<http://arXiv.org/ps/0704.1743v1>

This figure "figure10.jpg" is available in "jpg" format from:

<http://arXiv.org/ps/0704.1743v1>